RASĀYAN *J. Chem.*
307-313| Special Issue | 2022
ISSN: 0974-1496 | e-ISSN: 0976-0083 | CODEN: RJCABP
http://www.rasayanjournal.com
http://www.rasayanjournal.co.in

EXCELLENT SUPERCAPACITOR APPLICATIONS FOR ACTIVATED CARBON-BASED ZnO COMPOSITE BY GREEN SYNTHETIC METHOD

V. Raja[1], G. Selvan[1,✉], R. Anbarasu[1] and P. Ramanathan[2]
[1]PG and Research Department of Physics, Thanthai Hans Roever College (Autonomous) (Affiliated to Bharathidasan University, Tiruchirappalli), Perambalur-621220, T. N., India
[2]PG and Research Department of Chemistry, Thanthai Hans Roever College (Autonomous) (Affiliated to Bharathidasan University, Tiruchirappalli), Perambalur-621220, T. N., India
✉Corresponding Author: selvan96@rediffmail.com

ABSTRACT
ZnO nanoparticles will be combined with an activated carbon nanocomposite electrode to create a supercapacitor cell. The component measurement and rudimentary composition of NPs were resolute using TEM-SAED, and their optical transparency was investigated and TEM representation confirmed that the unit dimension was between 10 and 80 nm. Finally, the EI spectroscopy of ZnO and activated carbon is better considering its supercapacitor property. UV spectroscopy exposed an amalgamation signal at 372 nm, and the sample is transparent in the visible region at 5 mV/sec the conductance of the prepared sample is predictable to 185.2 F/cm^2. The electrochemical impedance of ZnO nanocomposites and activate carbon with dissimilar accumulation ratios (1:1 to 1:3) was measured, and the estimated capacitance value (was 185.2 F/cm^2).
Keywords: Activated Carbon, ZnO Nanocomposite, *Psidium guajava*, Supercapacitor, ZnO, TEM-SAED, UV-Vis Spectroscopy.

RASĀYAN *J. Chem.*, Special Issue, 2022
The Manuscript focusing SDG-9: Industry, Innovation and Infrastructure

INTRODUCTION

The ability of permeable carbonaceous electrodes is enhanced by oxides like ZnO, NiO, MgO, and RhO.[1-4] Partial conductor Nps are gaining global consideration owing to the enormous potential in bio applications and optoelectronics.[5-7] Specifically, semiconductors from the II-VI assembly contain be extensively used in bio and optoelectronic applications. ZnO is a visual and biocompatible feature with and band gap of 3.37 eV. In comparison to other metal oxide nanoparticles, ZnO cover recently predictable as a talented aspirant for bio-applications, including medical, industrial, and technical applications.[8] The morphology determines the bodily property with the intention of a second-hand multiplicity of application, resulting in the progress of a broad series of a method for synthesizing nanoparticles.[9] ZnO NPs contain excellent properties such as elevated ultraviolet incorporation, an extended lifetime, and an elevated surface-to-size fraction.[10] The high surface-to-size relation, medium[11], gas antenna[12], energetic stuffing for rubber and artificial, anti-virus representative within an outside layer and UV absorber surrounded by makeup[13-14], solar cell[15], varistors[16], and electrical and visual strategy.[17-22] Leaf takeout, therefore, is used as a plummeting agent in the Phyto mediated ZnO NPs. As a result, the present learn to develop a ZnO Nps with leaf extract using a green chemistry approach. This method has numerous advantages, including a low-cost precursor and a higher-purity, larger-quantity product. It doesn't need luxurious equipment and doesn't use any intermediate substances additional benefits include its speed and environmental friendliness.

EXPERIMENTAL

Groundwork of Leaf Extract

The plant *Psidium guajava* leaf was collected in Arumbavur, Perambalur District, India. They were cleaned with triple-deionized water before being cut into small pieces. 5 grams of fresh leaf pieces were extracted in a reflux condenser for 30 minutes with 100 ml deionized water. The extract was cooled to

http://doi.org/10.31788/RJC.2022.1558150

space temperature at about 30˚C.[23] Then, filter the solution with Whatman paper and refrigerate the filtrate for subsequent use.

Synthetic Route of ZnO

The newly prepared leaf extract mixture and the 1:4 zinc solutions were added and stirred at space temperature over 4 hours in conical flasks. 0.01 M $ZnNO_3$ solution. In a 110 °C burning atmosphere stove, the resulting accumulation was dehydrated. The yellow-colored glue was calcinated at 400 °C to get well crystals of ZnO-NPs, which were then stored in air-tight containers for further characterization. Figure-1 depicts the synthetic way for ZnO nanoparticles.

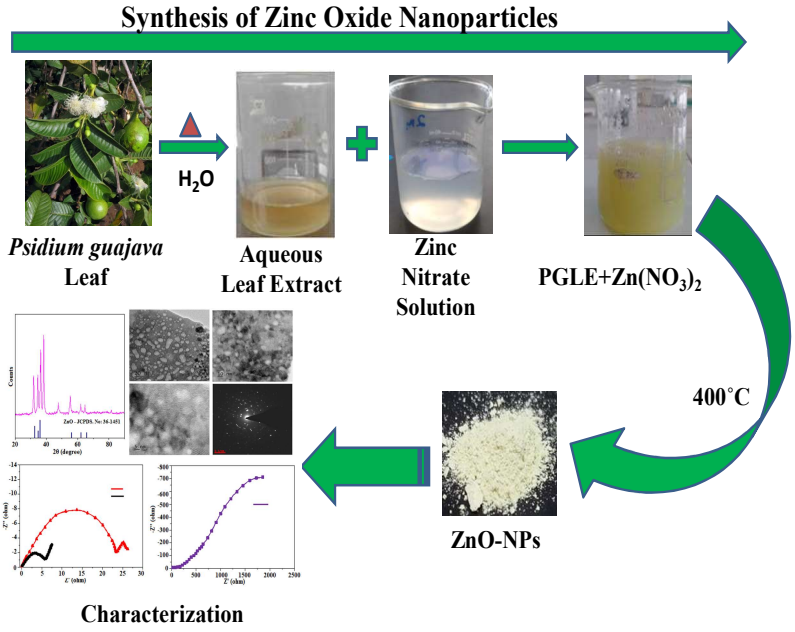

Fig.-1: Schematic Design of ZnO Nanoparticles

Production of Activated Carbon

To remove dust, soil, and suspended impurities, the leaf was washed numerous times with double distilled water. To build excellent particles, the material was ground with a pestle and mortar. A combination of 100g powdered fine materials and 50 ml con. H_2SO_4 was kept at space temperature for one day. To remove excess acid, the dried material was washed with double-distilled water. Finally, the fabric was dehydrated in a Stoppard bottle at 110 °C for 14 hours to remove moisture.

Production of Activated Carbon-ZnO Electrode

Activated carbon mixed with ZnO in multiple diverse proportions (1:3, 1:2, and 1:1) with the help of glue finished by combining n-methyl pyrrolidone and polyvinylidene fluoride. Following that, a brush was applied to AC-ZnO composite paste to a pre-weighted stainless steel power collector, which was then dried at 25°C.

Characterization of ZnO-NPs

UV-Vis spectrum and confirm the configuration of ZnO-NPs, a Shimadzu UV-1601 spectrophotometer was used. The FT-IR spectrum of HSLE was recorded in the KBr matrix by a BRUKER-FTIR-TENSOR-27 spectrophotometer with a frequency range of 400 to 4000 cm^{-1}. JEOL JSM 6390 was used to an acceleration voltage of 10 kV, the elemental composition of a Thermo EDX attachment. HR-TEM techniques were using a JEOL JEM 2100 instrument. The arrangement of ZnO was confirmed XRD SHIMADO-Model XRD 6000. The Nyquist curve was recorded using a CH electrochemical analyzer Model 604D. It was a three-electrode cell assembly that was used. Platinum and soaked calomel electrodes (SCE) were respectively used as counter- and reference electrodes. The electrode used was a composite electrode AC-ZnO. The EIS was used for electrochemical tests. Measurements of AC

impedances were performed using an AC signal with an amplitude of 5 mV of peak-to-peak range between 0.01 Hz and 100 kHz.

RESULTS AND DISCUSSION

Optical Spectral Analysis

UV is a dominant tool for investigating the arrangement of ZnO NPs in an aqueous solution. Figure-2 depicts the UV-Vis of leaf extract, $ZnNO_3$, and ZnO NPs. The formation is confirmed by the SPR band of ZnO-NPs at 372 nm. The swinging of free transmission band electrons excited by occasion electromagnetic radiation causes SPR absorption. While the assortment of the occasion light distances exceeds the wideness of the particles, this type of resonance is observed. The pointed peaks indicate the synthesized particles be of uniform size. This is consistent with previously published research on ZnO amalgamation signal at 374 nm[24-25] which proves the existence of ZnO nanoparticles.

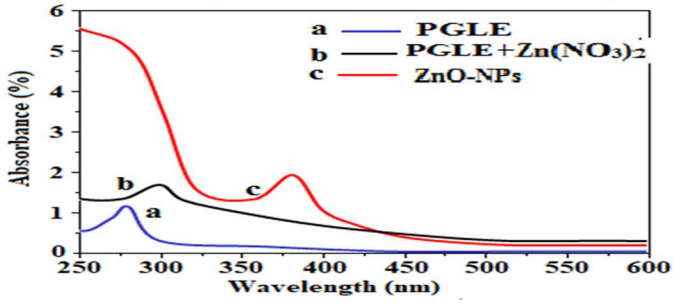

Fig.-2: The UV-Vis Range of Extract (a), Zinc Nitrate with Leaf Extract (b), and ZnO-NPs (c)

Functional Groups Analysis of ZnO-NPs

Figures-3a and 3b show the FT-IR of leaf mine and biosynthesized ZnO-NPs. FT-IR reveals several absorption bands at 3476, 1637, 1395, 1375, 1282, 1118, 1065, and 589 cm^{-1}, as well as other small bands. These bands match the –NH group, the C=O group, the C-H scissoring and twisting modes in hydrocarbon chains, the C=O broaden in C-O-C, the C-N stretching vibrations, and the aromatic carbon-carbon triple bond. ZnO NPs confirm a feeble amalgamation at 3480 cm^{-1} and 2929 cm^{-1}, which can be accredited to aliphatic asymmetric C-H stretching sensations and acid –C-H stretching. The peak at 1743 cm^{-1} corresponds to carbonyl group C=O vibrations. The peak of 672 cm^{-1} might accredit to CC vibrations. Vibrations of the M - O [Zn-O] bond are confirmed by the band at 483 cm^{-1}.[26]

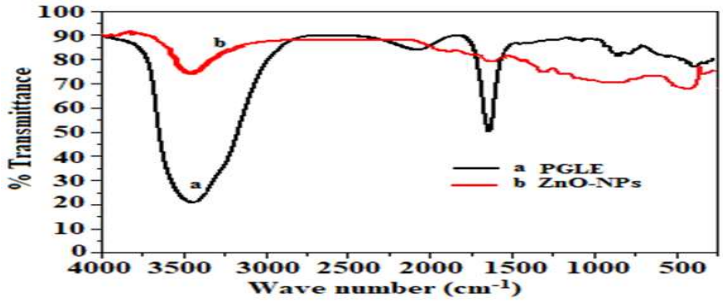

Fig.-3: FT-IR Band of PGLE (a) and *Psidium guajava* Mediated ZnO-NPs (b)

SEM and EDX Studies

The shape of nanoparticles can be predicted using an SEM analysis of leaf-mediated nanoparticles. Figure-4a shows the ZnO has a Wurtzite hexagonal shape by unit dimension range beginning 10 to 90 nm. Figure- 4b shows the EDX band of ZnO-NPs, which confirms the rudimentary composition of ZnO with 47% Zn and 53% O and no other signals present, representing the elevated clarity of synthesized ZnO-NPs.

HR-TEM Analysis

A TEM picture of ZnO-NPs is exposed in Figure-5. According to XRD data, the hexagonal (Wurtzite) shape of ZnO-NPs through atom sizes ranging from 10 to 80 nm is visible in the image. The

agglomeration of ZnO-NPs is caused by elevated exterior power owing to its synthesis in the aqueous medium, which results in a fine space between particles.[27] The SAED outline projects that the particle is extremely crystalline in nature, and an understanding of rings contain spots, indicating that the nanoparticles contain a uniform shape, larger granule size, and are polycrystalline in the scenery.

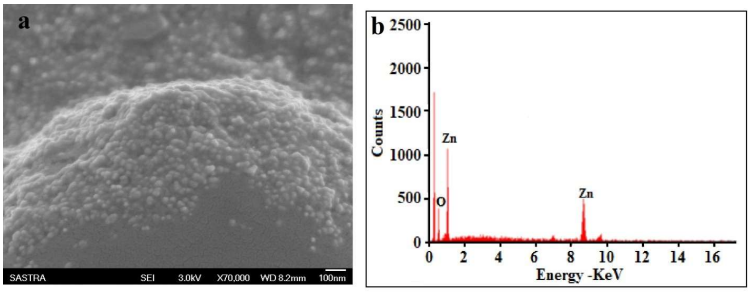

Fig.-4: (a) SEM Picture of ZnO-NPs, (b) EDX Spectra of Pure ZnO-NPs

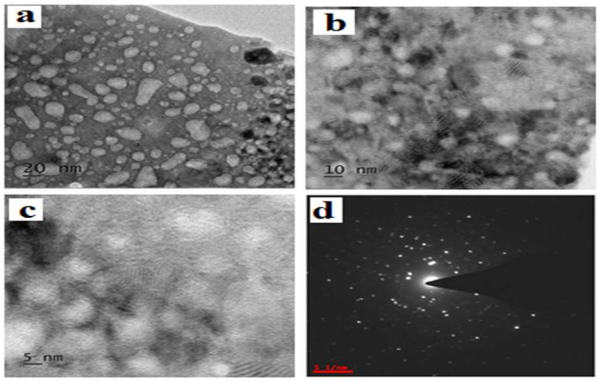

Fig.-5: HR-TEM Image of ZnO-NPs: (a) 20 (b) 10 (c) 5 nm and (d) SAED draft of ZnO-NPs

XRD Studies

As exposed in Fig.-6, the obtained diffraction peaks at 31.6, 34.2, 36.1, 47.5, 56.5, 62.7, and 67.9 correspond to miller indices of 100, 002, 101, 102, 110, 103, 112, 201, and 202, respectively. The results obtained show that the JCPDS file 036-1451 is well agreed.[22] The structure is confirmed to hexagonal Wurtzite structure. The clear and intense peak shows the crystalline personality of ZnO and its high purity. XRD prototype, the elevated - strength hit the uppermost point at the 101 planes is the distinguishing hit the utmost point of ZnO NPs and others diffraction peak does not recognized, indicating the clarity of ZnO-NPs.

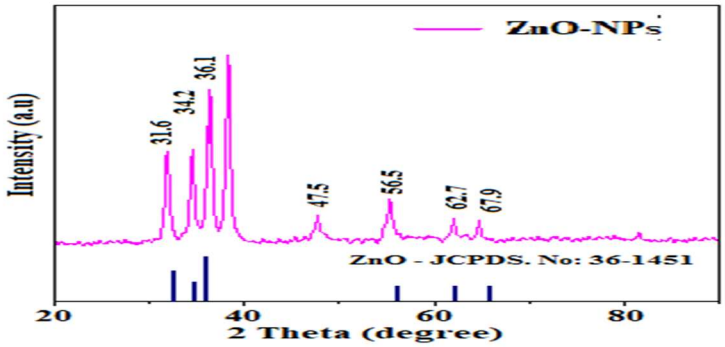

Fig.-6: XRD Patterns of ZnO-NPs

Electrochemical Impedance

A critical tool for the investigation of impedance with different ratios of AC-ZnO (1:3, 1:2, and 1:3) is examined with EIS. Figure-7 shows the Nyquist plots of AC-ZnO in 0.1 M Na_2SO_4 with two different ratios [1:3, 1:2]. In AC-ZnO (1:3 and 1:2), a distinct semicircle has been observed, implying a single

charge-transfer process between the working material and electrolyte. Table-1 shows the accuse relocation confrontation and specific capacitance ideals of AC-ZnO electrodes.

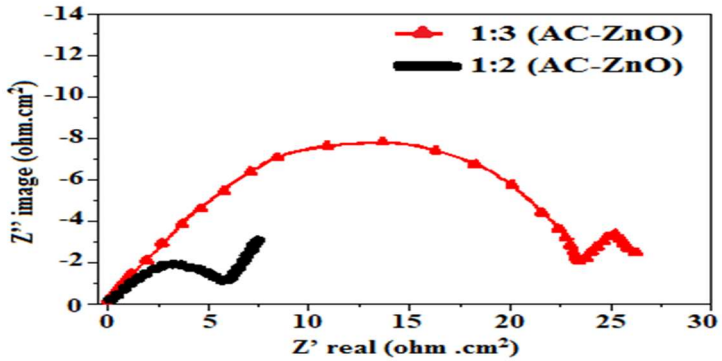

Fig.-7: Impedance Contrive for AC-ZnO Composites with 1:3 and 1:2 Compositions, With an Inset Showing the Equivalent Circuit Model

Table-1: Electrochemical Impedance Parameters for AC-ZnO electrode in 0.1 M Na_2SO_4

Materials	Scan rate (mV/Sec)	Charge transfer resistance (cm^2)	Capacitance (F/cm^2)
AC-ZnO (1:3)	5	25.1	7.4
AC-ZnO (1:2)	5	4.5	3.1
AC-ZnO (1:1)	5	2.1	185.2

The power relocation resistance increased as the ZnO content of the AC-ZnO composite mixture increased. Impedance diagrams for an AC-ZnO (1:1) electrode as a working electrode in 0.1 M Na_2SO_4 were obtained (Fig.-8). At little frequencies, a linear fraction is obtained, and at high frequencies, a half-moon is obtained. The capacitance worth increases at little frequencies owing to the large numeral of ions that move leading to a reduction in bulk resistance of the condenser.

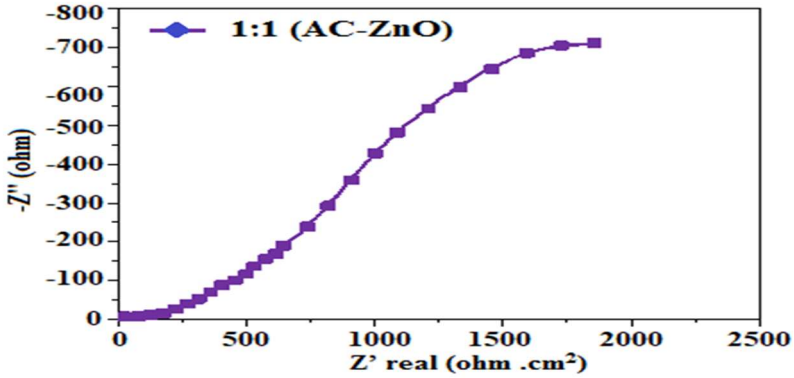

Fig.-8: Impedance Plots for AC-ZnO Composites at a 1:1 Mass Ratio

A parallel combination of strength and capacity is responsible for the half-circle, while Warburg impedance leads to the linear district. The linear area in the small frequency area relies more on the imaginary axis and shows a good ability to conduct. The distance of the half-moon (1:1 AC-ZnO) decreased when compared to the other two compositions (2:1 and 3:1 AC-ZnO), implying an increase in the available huge exterior area on AC-ZnO (1:1 ratio) and less restriction in the electron transfer process. As a result, the AC-ZnO composite electrode performs admirably as a supercapacitor in power storage space devices.

CONCLUSION

SEM and TEM, physical properties such as unit dimension series from 10 to 80 nm. They are also chemically examined using FT-IR, EDAX, and XRD, which reveal the existence of ZnO-NPs. An electrochemical presentation of activated carbon and ZnO composite combination was also investigated using EIS with 0.1 M Na_2SO_4 as the electrolyte at a inspect pace of 5 mV/s, the prepared AC-ZnO nanocomposite electrode has an exact conductance of 185.2 F/cm^2. The exact conductance of electrodes

decreases as the ZnO substance increases. The superior electrochemical presentation can be accredited to the elevated power conductivity of the trigger carbon and electroactive. Biosynthesized ZnO-NPs as supercapacitors after being composted with activated carbon. Supercapacitors have a high capacitance and supercapacitor active materials.

ACKNOWLEDGMENTS

The author acknowledges their thanks to St. Joseph's College, Tiruchirappalli, and Sastra University, Thanjavur, for providing analytical support. The author wishes to thank the Chairman, Principals, and faculty members of Physics, Thanthai Hans Roever College (Autonomous), Perambalur, Tamil Nadu for providing laboratory facilities and support.

CONFLICT OF INTERESTS

The authors declare that there is no conflict of interest.

AUTHOR CONTRIBUTIONS

All the authors contributed significantly to this manuscript, participated in reviewing/editing, and approved the final draft for publication. The research profile of the authors can be verified from their ORCID ids, given below:

V. Raja http://orchid.org/0000-0002-8980-6697
G. Selvan http://orchid.org/0000-0002-8980-6697
R. Anbarasu http://orchid.org/0000-0002-6333-7626
P. Ramanathan https://orcid.org/0000-0001-5894-722X

REFERENCES

1. E. Taer, M. Deraman, I.A. Talib, S.A. Hashmi and A.A. Umar, *Electrochimica Acta,* **56**, 10217(2011), https://doi.org/10.1016/j.electacta.2011.09.007
2. M.P. Bichat, E. Raymundo-Piñero and F. Béguin, *Carbon,* **48**, 4351(2010), https://doi.org/10.1016/j.carbon.2010.07.049
3. I. Stepniak and A. Ciszewski, *Journal of Power Sources,* **195**, 5130(2010), https://doi.org/10.1016/j.jpowsour.2010.02.032
4. B. Wen, S. Zhang, H. Fang, W. Liu and Z. Du, *Materials Chemistry and Physics,* **131**, 8(2011), https://doi.org/10.1016/j.matchemphys.2011.09.051
5. N. Singh, R.M. Mehra, A. Kapoor and T. Soga, *Journal of Renewable and Sustainable Energy*, **4**, 013110 (2012), https://doi.org/10.1063/1.3683531
6. S.J. Rosenthal, J.C. Chang, O. Kovtun, J.R. McBride and I.D. Tomlinson, *Chemistry and Biology,* **18**, 10 (2011), https://doi.org/10.1016/j.chembiol.2010.11.013
7. T. Jin, D. Sun, J.Y. Su, H. Zhang and H.J. Sue, *Journal of Food Science,* **74**, 46(2009), https://doi.org/10.1111/j.1750-3841.2008.01013.x
8. M. Li, Hari-Bala, X. Lv, X. Ma, F. Sun, L. Tang and Z. Wang, *Materials Letters,* **61**, 690(2007), https://doi.org/10.1016/j.matlet.2006.05.043
9. A. Ratkovich and R.L. Penn, *Materials Research Bulletin,* **44**, 993(2009), https://doi.org/10.1016/j.materresbull.2008.11.012
10. S.A. Akhoon, S. Rubab and M.A. Shah, *International Nano Letters,* **5**, 9(2015), https://doi.org/10.1007/s40089-014-0130-7
11. D. Yu, R. Cai, and Z. Liu, *Spectrochimca Acta - Part A, Molecular and Biomolecular Spectroscopy,* **60**, 1617(2004), https://doi.org/10.1016/j.saa.2003.09.003
12. M.L. Curri, R. Comparelli, P.D. Cozzoli, G. Mascolo and A. Agostiano, *Materials Science Engineering C,* **23**, 285(2003), https://doi.org/10.1016/S0928-4931(02)00250-3

13. A.K. Li, W.T. Wu, C.C. Kao and R.P.H. Chang, *Key Engineering Materials,* **247**, 405(2003), https://doi.org/10.4028/www.scientific.net/kem.247.405
14. H.M. Lin, S.J. Tzeng, P.J. Hsiau and W.L. Tsai, *Nanostructured Materials,* **10**, 465(1998), https://doi.org/10.1016/S0965-9773(98)00087-7
15. Z.S. Wang, C.H. Huang, Y.Y. Huang, Y.J. Hou, P.H. Xie, B.W. Zhang and H.M. Cheng, *Chemistry of Materials,* **13**, 678(2001), https://doi.org/10.1021/cm000230c
16. W. Jun, X. Changsheng, B. Zikui, Z. Bailin, H. Kaijin and W. Run, *Materials Science and Engineering B,* **95**, 157(2002), https://doi.org/10.1016/S0921-5107(02)00227-1
17. B.C. Feldmann, *Advanced Functional Materials,* **13**, 101(2003), https://doi.org/10.1002/adfm.200390014
18. R. Wu and C. Xie, *Materials Research Bulletin,* **39**, 637(2004), https://doi.org/10.1016/j.materresbull.2003.12.00
19. K. Se Lee, C. Woo Par, and J.D. Kim, *Colloids and Surfaces A Physicochemical and Engineering Aspects*, **555** (2018), https://doi.org/10.1016/j.colsurfa.2018.06.077
20. Y. Li and X. Liu, *Materials Chemistry and Physics,* **148**, 380(2014), https://doi.org/10.1016/j.matchemphys.2014.07.058
21. V. Raja, G. Selvan, R. Anbarasu and S. Baskar, *Indian Journal of Science and Technology,* **12(40)**, 1(2019), https://doi.org/10.17485/ijst/2019/v12i40/148040
22. C. Sohini, M. Amal Raj and N.L. Mary, *Journal of Energy Storage,* **28,** 101275(2020), https://doi.org/10.1016/j.est.2020.101275
23. A.A. Lawrence and J.T.J. Prakash, *International Journal of Science and Research,* **6**, 57(2018), https://doi.org/10.26438/ijsrpas/v6i6.5768
24. G. Sangeetha, S. Rajeshwari and R. Venckatesh, *Materials Research Bulletin,* **46**, 2560(2011), https://doi.org/10.1016/j.materresbull.2011.07.046
25. H. Abdul Salam, R. Sivaraj and R. Venckatesh, *Materials Letters,* **131**, 16(2014), https://doi.org/10.1016/j.matlet.2014.05.033
26. S. Azizi, M.B. Ahmad, F. Namvar and R. Mohamad, *Materials Letters,* **116**, 275(2014), https://doi.org/10.1016/j.matlet.2013.11.038
27. A. Becheri, M. Dürr, P. Lo Nostro and P. Baglioni, *Journal of Nanoparticle Research,* **10,** 679(2008), https://doi.org/10.1007/s11051-007-9318-3.

[RJC-8150/2022]